Supporting information for: Design of a Photoswitchable Cadherin

Ryan S. Ritterson, Kristopher M. Kuchenbecker, Michael Michalik, and Tanja Kortemme.

Table S1. Characterization of library mutants

Mutant	Conjugability*	Stability*	Switchability*	Half Life (min)	Change in Ca^{2+} - dependent binding upon illumination (SPR)
129/138	**High**	**High**	**80%**	**72**	**Significant**
70/14	Poor	High	51%	36	Non-Specific binding
70/107	High	High	100%	56	No Change
5/137	High	Poor	68%	44	No Binding
6/90†	Moderate	Poor	51%	ND	ND
111/135†	High	Moderate	62%	ND	ND
16/57†	High	Poor	45%	ND	ND
70/105†	ND	Poor	ND	ND	ND
70/133†	Poor	Poor	ND	ND	ND
95/139†	Very Poor	Moderate	ND	ND	ND
70/138†	Poor	Moderate	ND	ND	ND

ND: not determined.

* Conjugability was assessed qualitatively *via* mass spectrometry by noting the fraction that remains unconjugated. Stability was assessed qualitatively by noting appearance of protein precipitates or aggregation peaks during size exclusion chromatography. Switchability was assessed *via* absorbance assays (see Methods section).

† These mutants were tested with an earlier version of the EC12 construct that contains a non-native Met residue at the N-terminus (see Constructs section in Methods).

Figures

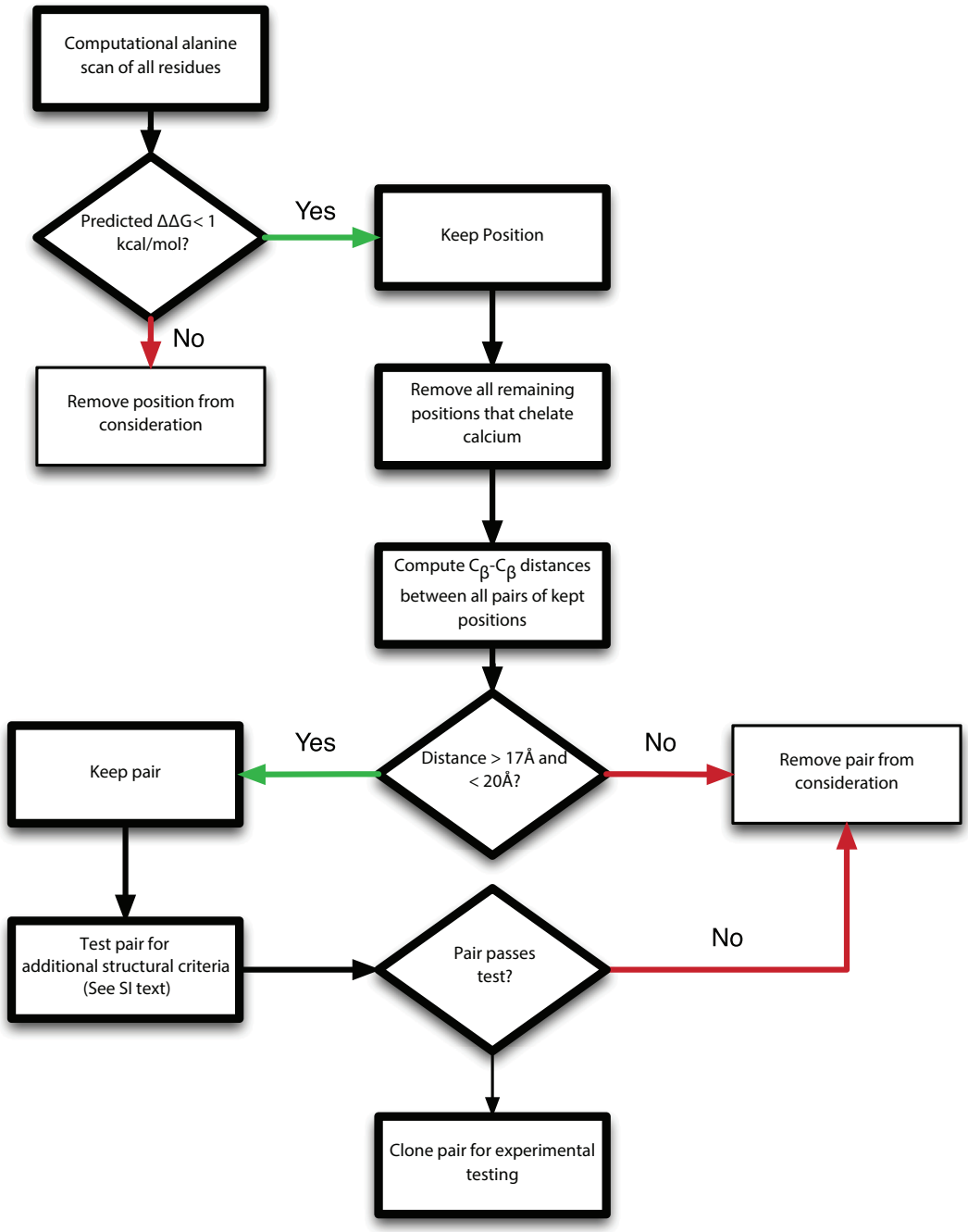

Figure S1. Flow chart showing the computational methodology used to create the mutant library.

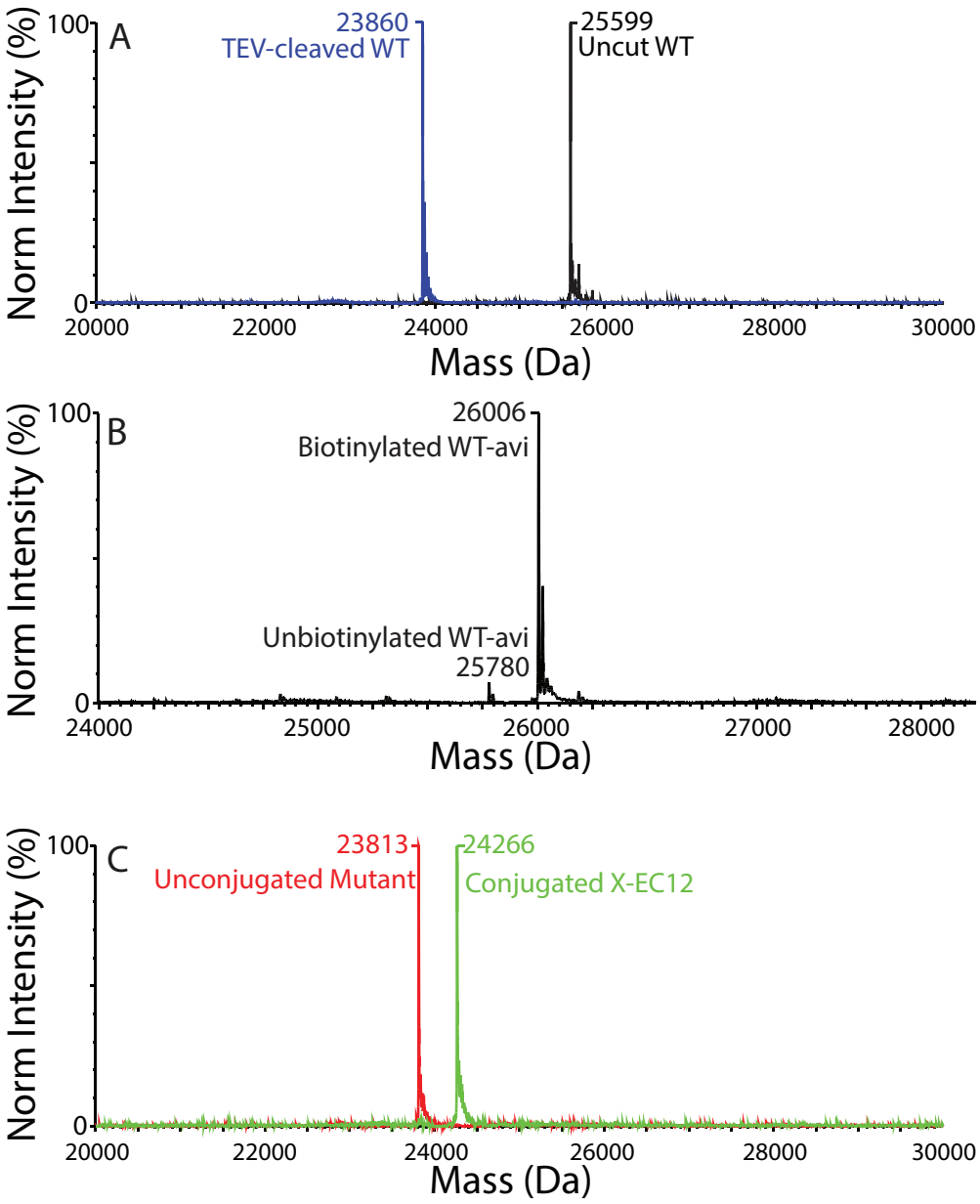

Figure S2. Mass spectra showing steps during protein production. A and C are overlays of two spectra. (A) Demonstration of mass change after cleavage. Black, uncut WT C9A protein; blue, WT C9A protein cleaved with TEV protease. Expected monoisotopic mass change was Δ1747 Da, compared to Δ1739 Da observed. (The difference could be due to imperfect protonation state prediction, such as for the 6xHis tag.) (B) Verification of Biotinylation. The majority of the protein is biotinylated. Expected and observed mass changes were both Δ226 Da. (C) Demonstration of mass change during conjugation: red, unconjugated mutant protein; green, conjugated mutant protein. Expected and observed mass changes were both Δ453 Da.

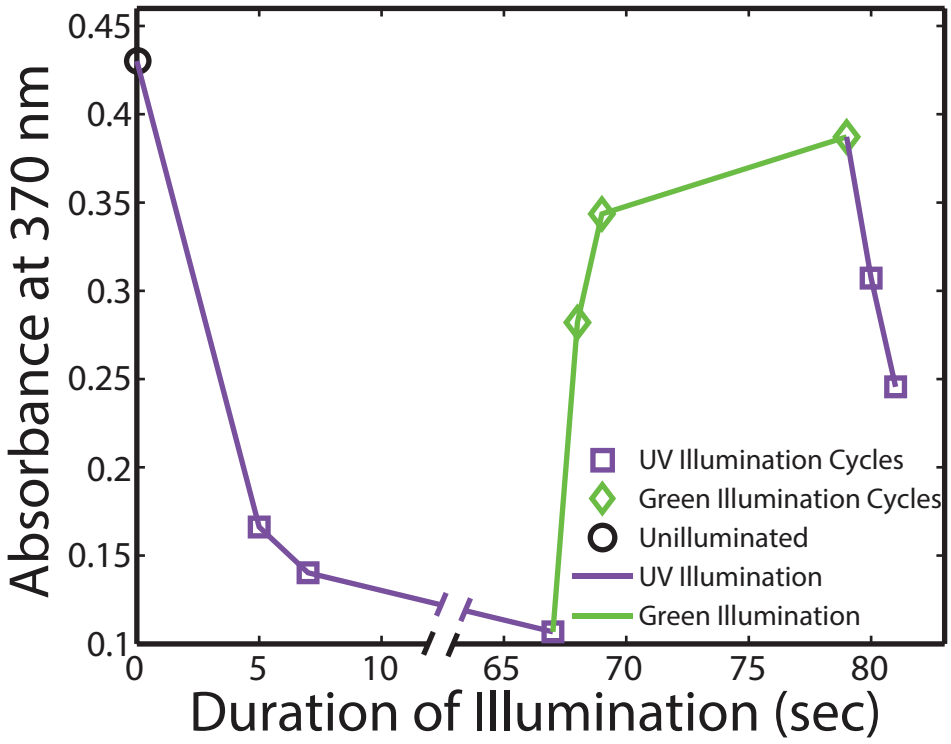

Figure S3. The extent of photoswitching is titratable. X-EC12 was illuminated with either UV light (purple lines) or green light (green lines) for various amounts of time, and the 370 nm absorbance was measured afterward. Shorter illuminations isomerize a smaller fraction of the protein.

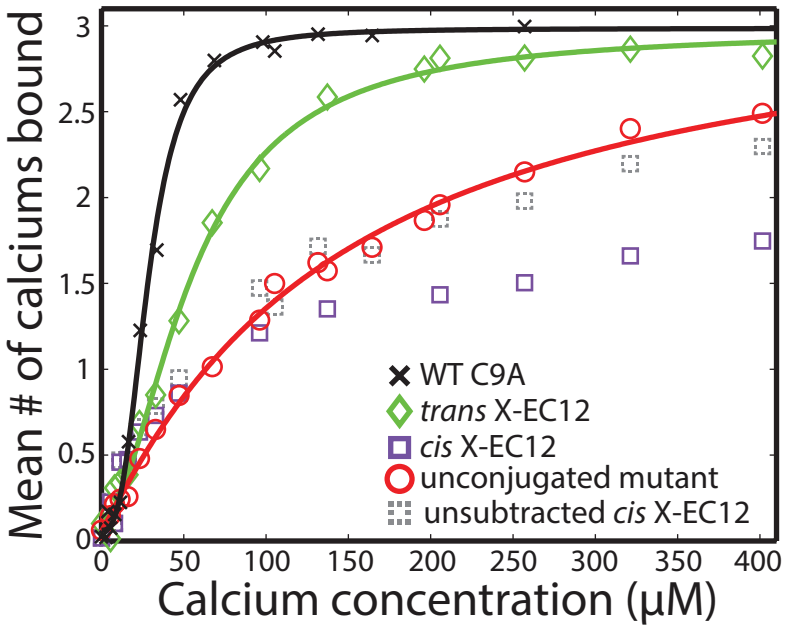

Figure S4. Calcium affinity as measured by mass spectrometry. Figure is the same as **Figure 2A**, with the addition of the *cis* state prior to subtraction of nonspecific binding (grey) and the unconjugated mutant (red). For the unconjugated mutant, K_d = 145 ± 18 μM and N_h = 1.07 ± 0.13. We speculate that the mutations increase the flexibility of the unconjugated protein, which weakens calcium binding affinity compared to WT. Subsequent addition of the *trans* crosslinker could re-rigidify the protein, allowing stronger calcium binding.

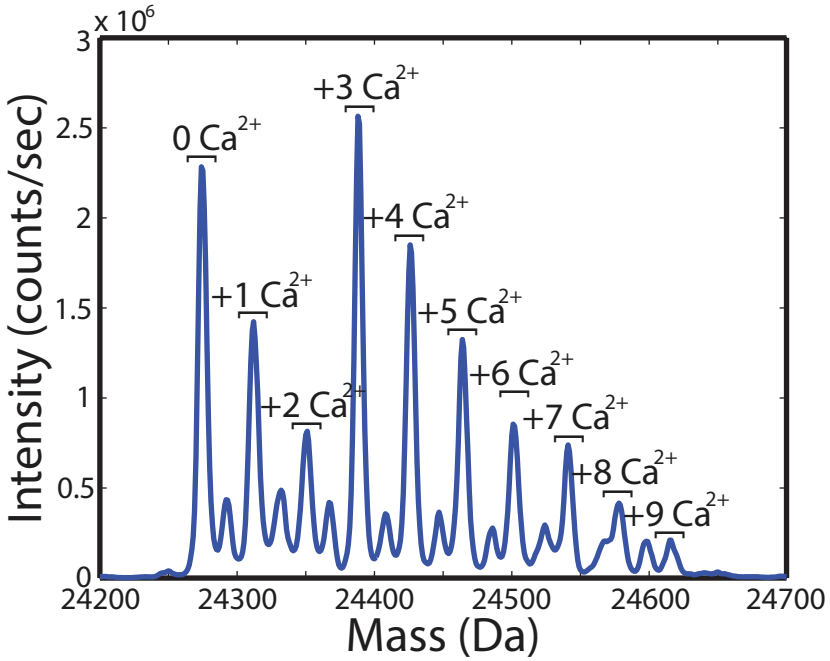

Figure S5. Example mass spectra showing calcium binding to *trans* X-EC12 at a calcium concentration of 96 μM. Unlabeled intermediate peaks are +1 Na.

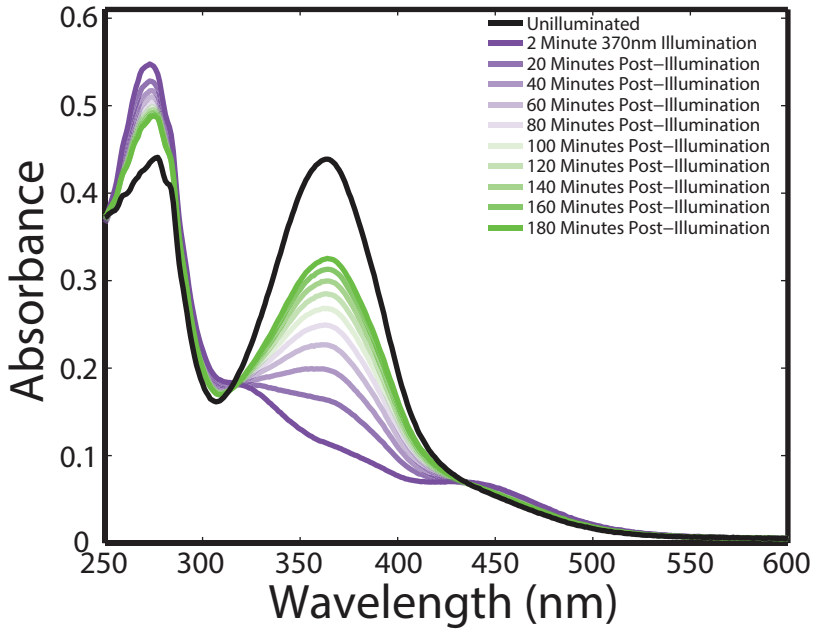

Figure S6. Illumination and relaxation of photoswitchable protein. Prior to illumination, X-EC12 is in the *trans* state (black). After illumination at 370 nm, much of the protein becomes *cis,* with a corresponding decrease in absorbance near 370 nm and a slight increase near 450 nm (darkest purple). Over time, *cis* X-EC12 relaxes to *trans*, with an increase in absorbance at 370 nm.

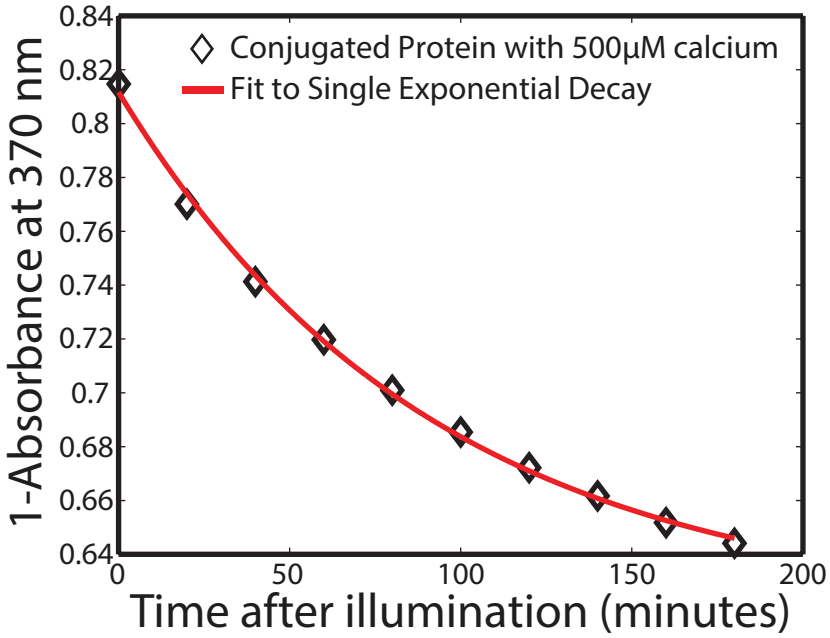

Figure S7. Example fit to single exponential of the relaxation of conjugated protein after illumination ($[Ca^{2+}]$ = 500 μM). For this illumination, the fit gave a half-life of 63.4 min.

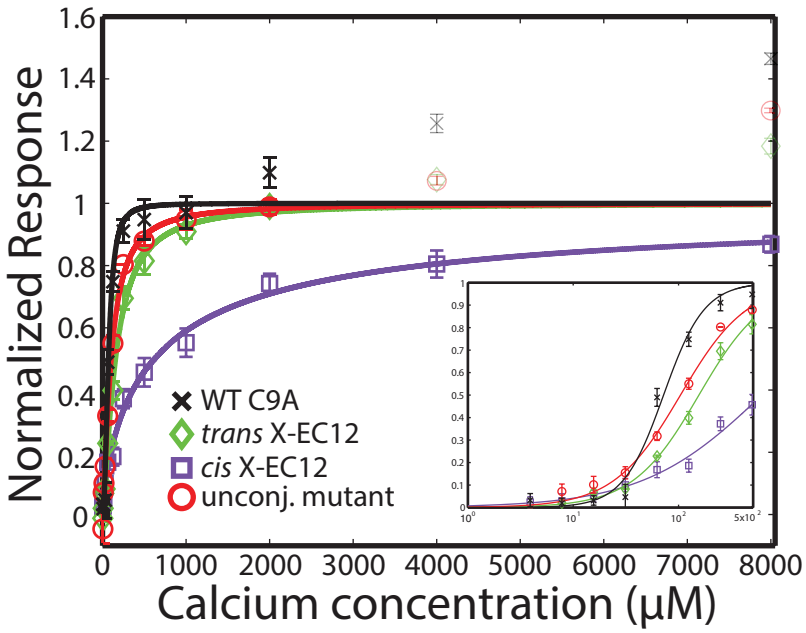

Figure S8. SPR calcium titrations as in **Figure 3A**, with the addition of the unconjugated mutant, red. For the unconjugated mutant, K_d = 104 ± 27 μM and N_h = 1.37 ± 0.47.

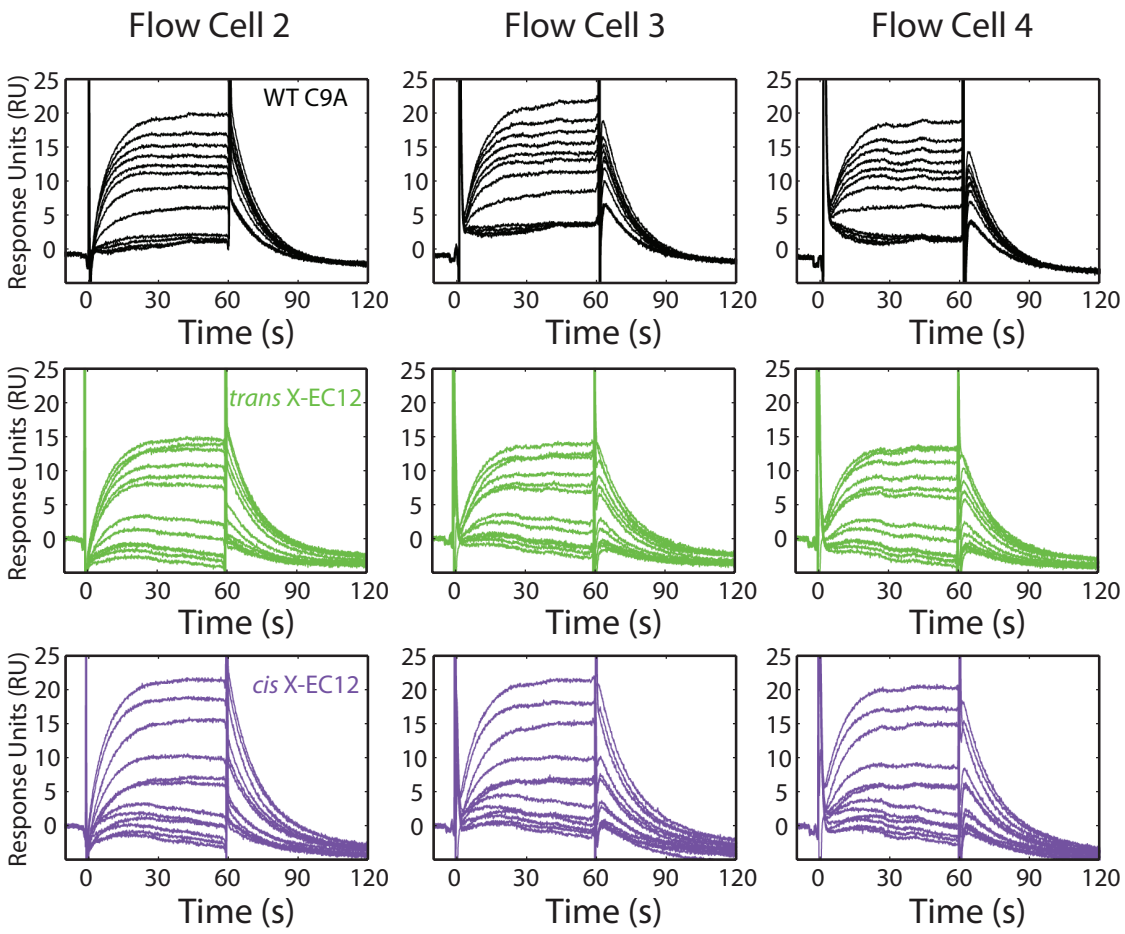

Figure S9. SPR traces from experiment in **Figure 3A**. Data are shown directly from instrument, prior to any post processing, blank subtraction, adjustment for surface response decay, scaling, or normalization. (Note: *cis* X-EC12 was collected first, leading to a higher response than *trans* X-EC12 due to surface decay)

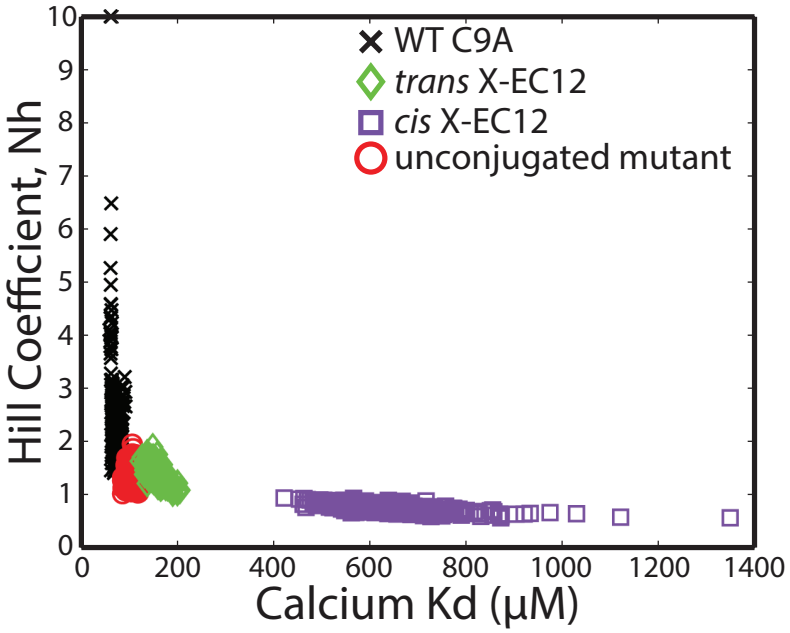

Figure S10. Plot of values resulting from the bootstrap analysis of the SPR calcium titration data. All 500 points for each protein plotted.

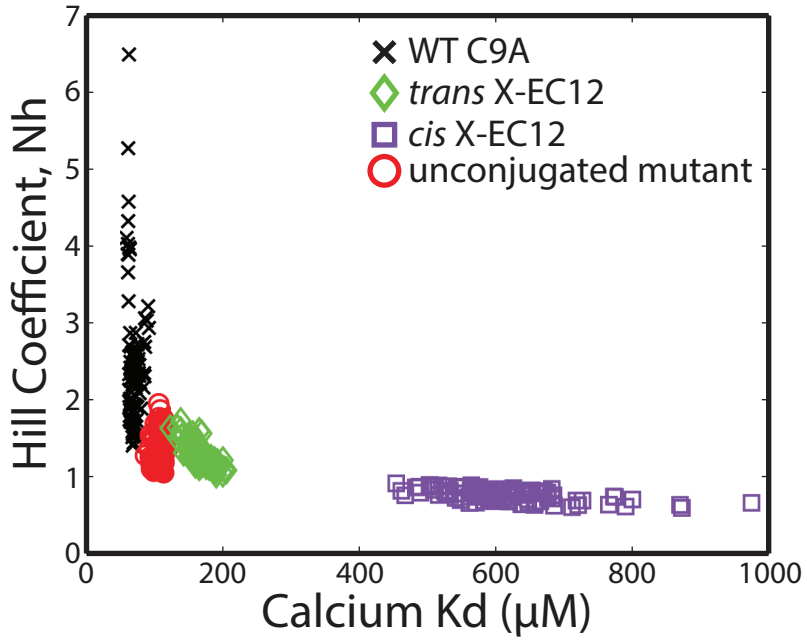

Figure S11. Plot of values resulting from the bootstrap analysis of the SPR calcium titration data. Only shown are the top 100 points by minimum sum of squared error (SSE) for each protein used to compute the mean and ±2 SD values.

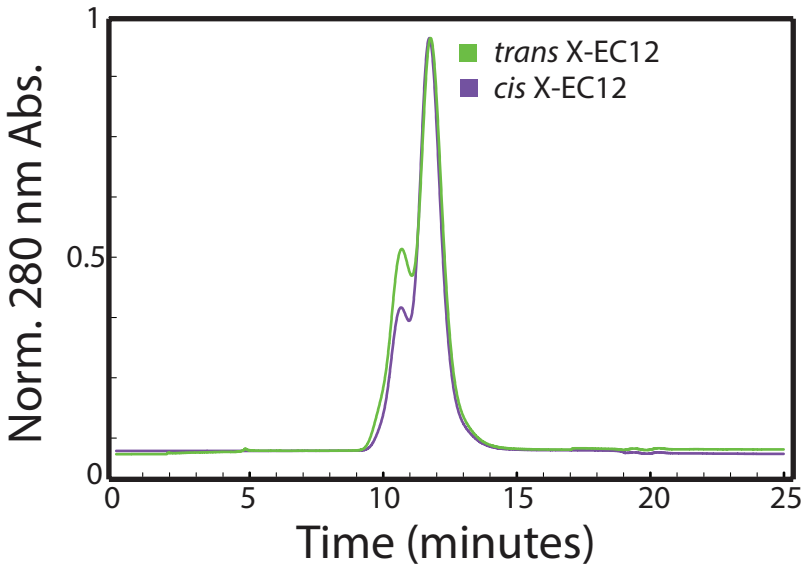

Figure S12. Size exclusion chromatography of *cis* and *trans* X-EC12. Injected samples contained 250 μM protein and 2500 μM Ca^{2+}. Chromatograms have been normalized to the height of the largest peak (the monomer) to allow easier comparison of relative peak fractions.

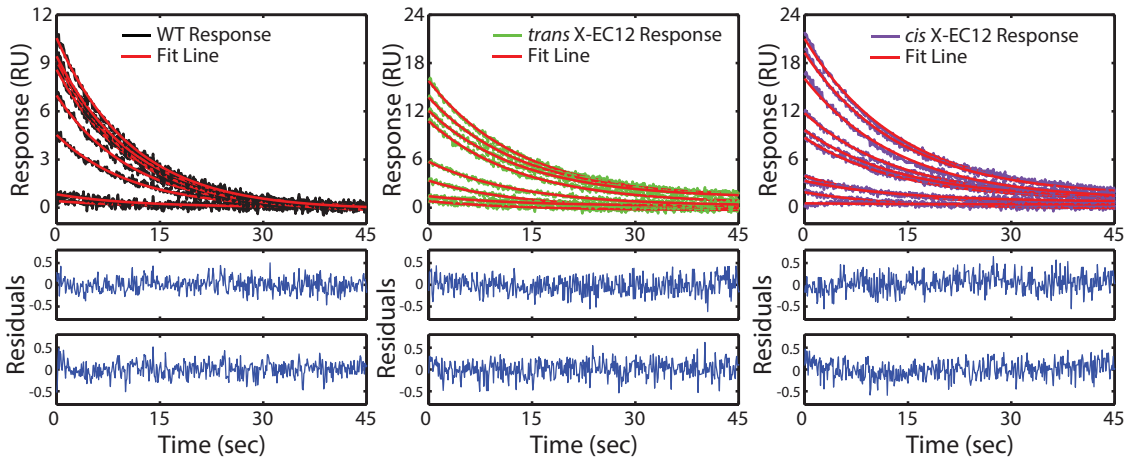

Figure S13. Dissociation of cadherin dimers from experiment in **Figure 3A**. Top panels show dissociations and fits with a common off rate to a single exponential for each protein. Bottom panels show representative residuals of fits, shown for $[Ca^{2+}]$ = 62.5 μM (upper) and 1000 μM (lower). Reponses are from flow cell 2.

Methods

Design Methodology

As described in the main text, the design problem here can be reduced to finding the best pair of cysteine attachment sites for the chromophore, such that when conjugated, the system both maintains its native function, but also shows high switchability and functional changes when illuminated. (**Figures 1C** and **S1**) Our design process involved first finding residues likely to be mutatable using the computational design program Rosetta.[1] We used a previously described method[2,3] to predict the change in fold stability of mutating, one by one, every residue in four representative E-cadherin structures (PDB identifiers 1FF5, 1EDH, 2O72 and 1Q1P) to alanine, the simplest mutation. Residues that had an average predicted change in fold stability > 1 kcal/mol upon alanine mutation were removed from consideration. We also removed all residues that directly bound calcium from consideration, reasoning that mutating them would likely cause a significant change in cadherin's calcium affinity. Next, we calculated all pair-wise C_β-C_β distances between the residues remaining using the 1FF5 structure, and kept those pairs that fell in the range 17-20 Å (appropriate for the BSBCA *trans* isomer). These first two steps reduce the potential double mutants from >20000 pairs to 1513.

Following these initial steps, we further restricted the number of pairs via a series of additional structural criteria. First, we restricted the remaining pairs to those that had at least one endpoint within 20 Å of a calcium ion as measured by the molecular graphics program PyMol[4], reasoning that pairs with both ends distant from the calcium binding sites would be unlikely to have an effect on calcium binding. This further reduced the

number of pairs to 1120. Next, to only use residues that were accessible for chromophore conjugation, we restricted pairs to those where both endpoints were in residues that had >30 $Å^2$ of solvent accessible surface area (SASA) when the protein was in the monomeric state, again measured using PyMol. This reduced the set of pairs to 272. Finally, we plotted the remaining pairs on the 1FF5 PDB structure and eliminated those where the addition of the chromophore would sterically interfere or clash with the native protein structure, as estimated by using the surface representation of the protein structure and eliminating those pairs whose path of shortest distance penetrated the surface. This step eliminated a large part of the remaining set, leaving 28 pairs of conjugation sites. As a final step, we manually examined the 28 pairs and chose a set of 10, seeking to build a diverse set of conjugation sites to maximize the chances of finding a functional photoswitch. One mutant pair, P5C/D137C, did not satisfy the structural criteria; it was chosen manually in an attempt to construct a photoswitch coupled to β-strand one, based on the previously observed functional importance of the strand to cadherin dimerization.[5,6]

Constructs

Natural E-cadherin contains a pro-peptide cleaved during protein maturation, leaving an N-terminal aspartate residue instead of a methionine. This aspartate forms an important intramolecular salt bridge, resulting in recombinantly produced proteins containing an N-terminal methionine having altered function.[7] To remove both the exogenous 6x-His tag and methionine, we introduced a TEV protease cleavage site. TEV protease is compatible with the reducing buffer conditions (containing 3 mM TCEP)

required to maintain free cysteines in our engineered constructs prior to conjugation, whereas other common proteases are not.

Met-EC12-6xHis was cloned into pET-22b(+) (EMD Millipore # 69744-3) as described previously.[8] 6xHis-TEV-EC12 contained a 6xHis tag and TEV cleavage site (ENLFYQ) added N-terminally, as well as an inserted C-terminal stop codon between EC12 and the C-terminal 6xHis tag using the 5' oligonucleotide (GACCCCATATGCACCACCACCACCACCACGAAAACCTGTACTTCCAGGGGA CTGGGTC) (blue-6xHis, orange-TEV cleavage site) and the 3' oligo (TGGTGCTCGAGTCAAGGAGCGTTGTCA). For 6xHis-TEV-EC12-avitag, the same 5' oligo was used, and the 3' oligo was replaced with one containing both an AviTag[9] and stop codon (TGGTGCTCGAGTCATTCGTGCCATTCGATTTTCTGAGCCTCGAAGATGTCGTT CAGACC GCCACCAGGAGCGTTG). (green-*avitag*) The resulting PCR products were then re-inserted into pET-22b(+) using the same procedure as before.

Protein Expression and Purification

Protein Expression 6xHis-TEV-EC12 and Met-EC12-6xHis were expressed in *E. coli* BL21(DE3) cells as described previously,[8] with the substitution of 100 µg/mL carbenicillin replacing ampicillin. The 6xHis-TEV-EC12-avitag construct was co-transformed into BL21(DE3) cells with a plasmid containing biotin ligase (Gift from R. Fletterick). Protein was expressed under the same conditions as 6x-TEV-EC12 with the addition of 34 µg/mL chloramphenicol and 50 µM biotin (Thermo #29129) to LB culture medium. (BD #244610)

Lysis Cells were resuspended at 20 mL/L of culture in lysis buffer (50 mM Tris-HCl pH 8.0, 2.5 mM $MgCl_2$, 0.1% Triton X-100). After resuspension, protease inhibitor tablets (Roche #11836170001) were added according to manufacturer's instruction. After addition of 1U/mL of DNAse I (NEB #M0303) and 0.1 mg/mL lysozyme (Sigma #L6876), resuspended cells were stirred for 1 hour at room temperature. Cells were subsequently lysed using sonication, then lysates were cleared by centrifugation at 21,000x*g* for 30 minutes at 4 °C. (*Note: In our hands, EC12 is prone to aggregation if NaCl is present in the lysis buffer prior to clearing of lysates.*)

Ni-NTA Purification After lysis, NaCl and imidazole were added to final concentrations of 300 mM and 10 mM, respectively, followed by 50% NiNTA agarose slurry (Qiagen #30230) at a volume of 5 mL/L of culture. Lysates were then nutated at 4 °C for 1-2 hours, and beads were pelleted by spinning at 3000x*g* for 10 minutes. Beads were resuspended in wash buffer (50 mM NaH_2PO_4-NaOH pH 8.0, 300 mM NaCl, 10 mM imidazole), separated *via* a gravity-flow chromatography column (BioRad #732-1010), then further washed *via* 2 column volumes (CV) of wash buffer. Protein was eluted from the beads using 1.25 CV elution buffer (50 mM NaH_2PO_4-NaOH pH 8.0, 300 mM NaCl, 250 mM imidazole). Eluted protein was injected into a HiLoad 16/600 Superdex 75 column (GE #28-9893-33) attached to an FPLC system and prequilibrated in TEV cut buffer (25 mM TrisHCl pH 8.5, 400 mM NaCl, 1 mM EDTA, 3 mM KCl, 3 mM TCEP). Monomer fractions were pooled. Typical yields of monomer ranged from 10-20 mg protein per liter of cell culture.

Protease Cleavage and Repurification

Cleavage Purified proteins were concentrated to a final concentration of 120 μM in TEV cut buffer using spin concentrators (Millipore #UFC901024) (*Note: In our hands, EC12 adsorbs to alternative protein concentrators*), after which 6xHis-TEV (Invitrogen #12575-015) was added in a mass ratio of 1:8 TEV:EC12. Protease reactions were left at 16 °C for 60 hours.

Repurification After cleavage, protease, tags, residual contaminating proteins, and residual uncleaved protein were removed using a second round of NiNTA purification. The protease reactions were desalted using a HiPrep 26/10 desalting column (GE #17-5087-01) into repurification buffer (25 mM Tris-HCl pH 8.0, 400 mM NaCl, 30 mM imidazole, 500 μM TCEP). After desalting, Ni-NTA agarose pre-washed in repurification buffer was added at a ratio of 1mL of packed resin per 15 mg EC12 and mixtures were nutated for 1-2 hours at 4 °C. After nutating, supernatants containing cleaved protein were separated from beads using a gravity-flow chromatography column. Beads were washed using 1CV repurification buffer, and wash fractions were pooled with supernatants. Proteins were then desalted into TEV cut buffer for medium term storage. Protein purity was verified by SDS-PAGE and was estimated to be > 90% and cleavage completeness was verified *via* mass spectrometry. (**Figure S2A**) Biotinylation efficiency was also verified *via* mass spectrometry. (**Figure S2B**) Typical yields post-repurification were 66-75% compared to precleavage, with the major loss being incomplete cleavage. Biotinylation was typically >95% of overall protein.

Conjugation

3,3'-bis(sulfonato)-4,4'- bis(chloroacetamido)azobenzene

(BSBCA) Handling Dry BSBCA (purchased from Linkera-osadovsk@chem.utoronto.ca) was kept at 4 °C. 16X stock solutions were created by dissolving dry BSBCA into water at a concentration of 8 mM. Stock solutions were kept at -20 °C in the dark.

Protein Conjugation Repurified and cleaved mutant protein was concentrated to a final concentration of 160 μM in TEV cut buffer, followed by addition of BSBCA from stock solutions to a final concentration of 500 μM. Conjugation reactions were kept in the dark at 25 °C for 72 hours. After conjugation, excess chromophore was removed *via* desalting using a HiPrep 26/10 desalting column (GE #17-5087-01) into TEV cut buffer. Conjugation efficiency was verified using mass spectrometry, looking for the characteristic increase of 453 Da[10], and efficiencies were typically >99% for the mutant K129C/D138C. (**Figure S2C**) (*Note: Free chromophore has a tendency to adsorb to the resin, especially in the presence of salt. It may be removed by flushing the column with several volumes of pure water.*)

Final Purification & Storage

Prior to analysis, proteins were injected into a HiLoad 16/600 Superdex 75 column equilibrated in storage buffer (25 mM Tris-HCl pH 7.5, 150 mM NaCl, 500 μM TCEP) to remove any aggregates that may have developed during cleavage, repurification or conjugation. Typical monomer yields were 90% for unconjugated and 60% for conjugated protein. Proteins were stable in storage buffer for several weeks at 4 °C. For longer term storage, proteins were flash frozen in storage buffer containing 10% v/v glycerol using liquid nitrogen, then stored at -80 °C. (*Note: Conjugates had a high non-specific affinity for agarose and other common support matrices. Attempts to conjugate protein prior to cleavage and repurification led to protein aggregation. Attempts to*

separate TEV from conjugated EC12 using other column methods such as protease-affinity columns were similarly unsuccessful. Conjugated protein remains monomeric in the Superdex 75 and HiPrep Desalting columns used here.)

Protein Concentration Determination

Unconjugated protein concentrations were determined using measurements of absorbance at 280 nm using extinction coefficients predicted by the ExPASY online protein parameter tool[11], which were ε_{280}=21430 M^{-1} cm^{-1} for EC12, and ε_{280}=26430 M^{-1} cm^{-1} for EC12-avitag. For conjugated proteins, the extinction coefficient at 280 nm was computed as the sum of the predicted protein and measured free BSBCA (ε_{280}=10100 M^{-1} cm^{-1}) extinction coefficients. BSBCA's extinction coefficient was computed by measuring BSBCA's absorbance at 370 nm and 280 nm and using

$$\varepsilon_{280} = \frac{A_{280}}{A_{370}} * \varepsilon_{370} \quad (1)$$

where ε_{370}= 29000 M^{-1} cm^{-1} (see Zhang et al.[12]). BSBCA's molar extinction coefficients can vary when conjugated to protein. However, similar band intensities were observed when conjugated and unconjugated proteins of identical computed protein concentration were loaded into an SDS-PAGE gel and then stained with coomassie.

Conjugability Measurements

Post conjugation, conjugation reactions were diluted to a final protein concentration of 1 μM in pure water, and then analyzed *via* mass spectrometry using an LCT Premier (Waters). (**Figure S2C)** We observed the peak ratio between the unconjugated and

conjugated (+453 Da) peaks, and, assuming equal ionizability for each species, made a qualitative determination of conjugability. (**Table S1**) Highly conjugatable mutants showed only trace remaining unconjugated proteins, whereas poorly conjugatable mutants showed as little as 10% estimated conjugation.

Switchability Measurements

For each cadherin double mutant, we determined whether the BSBCA conjugated to the protein was photoisomerizable by illuminating *trans*-relaxed X-EC12 with UV light. *Trans* BSBCA contains a characteristic absorbance peak near 370 nm, and, upon illumination at that wavelength, the peak amplitude decreases as the small molecule isomerizes into the *cis* state.[13] Data provided to us by Dr. Andrew Woolley,[14] containing extinction coefficients for conjugated proteins separated by HPLC, containing isolated *trans* or *cis* isomers allowed us to estimate the fraction of EC12 that switched to *cis*. By assuming the observed 370 nm absorbance of any mixture of *cis* and *trans* can be described by the simple sum of the independent absorbances of the underlying *cis* and *trans* states, switching percentages can be calculated by

$$Frac = \frac{\varepsilon_{370nm,trans} - \varepsilon_{370nm,mix}}{\varepsilon_{370nm,trans} - \mathrm{R} * \varepsilon_{370nm,trans}} \quad (2)$$

Here, R is the *cis/trans* extinction coefficient ratio computed from the provided data (.0541), $\varepsilon_{370nm,trans}$ is the measured extinction coefficient at 370 nm for the thermodynamically equilibrated, 100% *trans* state, and $\varepsilon_{370nm,mix}$ is the measured extinction coefficient at 370 nm for the photostable, UV illuminated state containing a

mixture of *cis* and *trans*. Using this methodology, we computed a switchability for the free chromophore of 86% *cis,* close to published estimates of maximum switchability.[13]

Calcium Binding Measurements

Protein samples were prepared as previously described[15], with the modification that samples were diluted to 2 pmol/μL. Samples were injected at 5 μL/min into a QTRAP4000 instrument (Agilent). *Cis* X-EC12 was illuminated with a 1 W UV LED (Advancemart, emission maximum 365 nm) for 4 minutes immediately prior to injection. The quantity of bound calcium ions was obtained by determining Ca^{2+} binding occupancies, and assuming that calcium-free and calcium-bound molecules have the same ionizability.[16] By comparing peak areas, fractions of molecules binding 0 to 9 calcium ions were computed for each calcium concentration (**Figure S5**). For determination of K_d, molecules binding more than three calcium ions were assumed to bind three ions specifically, and these fractions were added to the 3-ion fraction. The average number of calcium ions bound was computed, and the resulting numbers were fit to a Hill equation.[17] In order to subtract non-specific binding from *cis* X-EC12, the following equation was used for each calcium concentration, *i,* and occupancy number, *c*:

$$F_{c,i} = \dot{F}_{c,i} - \left(\sum_{a=1}^{c} \dot{F_{c,\iota}} * x_{a,i} \right) + \left(\sum_{a=1}^{\min(9-c,6)} \dot{F}_{c+a,i} * x_{a,i} \right) \quad (3)$$

where $F_{c,i}$ is the true fraction of the molecules binding *c* specific calciums at concentration *i*, $\dot{F}_{c,i}$ is the apparent fraction binding *c* calciums at concentration *i*, and $x_{a,i}$ is the fraction of the molecules that bind *a* non-specific calciums at concentration *i*. The

first summation in the equation subtracts from the apparent fraction contributions due to non-specific binding, whereas the second term adds from the other calcium occupancy states their non-specific fractions that actually bind *c* calciums. The non-specific binding fractions, $x_{a,i}$, came from the *trans* X-EC12 calcium series using the assumption that all three calcium binding sites were occupied prior to non-specific sites, thus any fraction that appeared to bind four calciums actually bound three specific and one non-specific calcium, etc.

Isomerization Relaxation Measurements

Conjugated proteins in storage buffer at 12 μM were illuminated with the same 1 W UV LED for 4 minutes and the absorbance at 370 nm was monitored immediately after illumination and then every 20 minutes thereafter for a total of 180 minutes (**Figure S6**). The absorbances were blank subtracted and then each absorbance was subtracted from 1.0 and the combined numbers were fit to a single exponential decay function of the form $y = A * e^{-bx} + c$ using the curve fitting toolbox in MATLAB (The MathWorks) (**Figure S7**). R^2 values were typically >.995. Half-lives were computed as $\lambda = {\ln(2)}/{b}$. For the calcium dependence of half-life, proteins were illuminated, and then $CaCl_2$ was added to final concentrations from 3.9 μM to 32 mM, using a 14-point 1:1 serial dilution series, plus a zero calcium point. Data points were collected five at a time on a Cary 50 Bio UV/Vis spectrometer (Varian), and the entire series was run in triplicate. The mean half-lives for each calcium concentration were plotted and fit to a Hill curve of the form

$$y = \left({bx^{N_h}}/{c^{N_h} + x^{N_h}}\right) + d \quad (4)$$

using the curve fitting toolbox in MATLAB, where N_h is the hill coefficient and c is the EC_{50} for calcium-dependent half-life reduction. Absorbance curves were also fit to double exponentials, without a significant increase in curve quality (Data not shown).

Isomerization Reversibility

Conjugated protein at 12 μM in storage buffer was illuminated using the same UV LED for 2 minutes and 370 nm absorbance was measured. After measurement, protein was illuminated with a 1 W LED (Sparkfun, emission maximum 455 nm, with residual intensity in the 500-550nm range) for 2 minutes, 370 nm absorbance was measured, and the process was repeated for 10 cycles.

Surface Plasmon Resonance (SPR)

Data acquisition Matrix-free, flat, carboxymethylated gold surfaces (GE Healthcare Sensor Chip C1) were used in all SPR experiments. Individual flow cells were prepared with the following protocol: (1) 50 μl injection of 1-Ethyl-3- (3-dimethylaminopropyl)carbodiimide / N-hydroxysuccinimide (0.5M:0.2M); (2) 30 μL injection of 0.25 mg ml-1 ImmunoPure Streptavidin (Pierce #21122) in sodium acetate buffer (pH 5.0) to a total amount of ~500 response units (RU) for all four flow cells; (3) 60 μl injection of 1 M ethanolamine. Cadherin was captured on the active flow cells by manual injection of 25 nM protein to immobilization levels between 250-450 RU. No blocking procedures were performed on the reference flow cell. Prior to each SPR experiment, protein samples were dialyzed against 25 mM Tris, 150 mM NaCl, and 500 μM TCEP. Following dialysis, Tween 20 detergent (Sigma-Aldrich #P9416) was added to the protein solution and the dialysis buffer to achieve a final concentration of 0.05%

(v/v). The dialysis buffer was then used as the assay buffer for the SPR measurements. Dose response titrations were prepared by serial dilutions of the highest concentration into assay buffer. While measuring *cis* X-EC12, a maximum of three data points per illumination cycle were used, to maximize *cis* fraction and minimize thermal relaxation. To minimize systematic error due to some fraction of the protein reverting to *trans* during the experiment, concentrations were injected in a random order. For all samples, injection was followed by a control injection of 20 μM WT C9A cadherin containing 1mM $CaCl_2$ to monitor degradation of chip response over time. Each sample response was subtracted by a reference response (containing no calcium for calcium titrations, and no protein for protein titrations), and then corrected in magnitude by the magnitude of the control injection. Raw SPR traces are shown in **Figure S9**. The responses of flow cells 2 and 3 were scaled to match flow cell 4 *via* a least squares minimization resulting in a single scalar multiplier for each flow cell. Each titration series was then fit to an equation of the same form as eq 4, where here c is the EC_{50} for calcium-dependent protein binding using the curve fitting toolbox in MATLAB. Due to chip-to-chip variation, calcium binding fits were normalized such that the maximum responses at infinite concentration predicted by the fit lines were equal to one. During calcium titrations, we observed an EC_{50}-dependent, non-specific interaction at higher calcium concentrations, with a stronger (lower) EC_{50} leading to a larger magnitude effect (i.e. WT C9A had the strongest effect, *cis* X-EC12 had no apparent effect at concentrations tested). Points dominated by this effect were not used in the fits, but are shown as faded markers in **Figures 3** & **S8**. For reversibility analysis, 40 μM X-EC12 was alternatingly illuminated with UV (emission maximum 365 nm) and blue LEDs (emission maximum 455 nm, with residual intensity at 500-550 nm),

1mM Ca^{2+} was added, and responses measured. The resulting responses were subject to the same reference and control subtraction, as well as flow cell scaling used in the calcium titrations.

Bootstrap analysis We used a bootstrapping technique in order to verify fit values were robust. Data points for each flow cell and concentration were grouped, and then data points were drawn at random, with replacement, in a number equal to the number of actual data points. These randomly drawn data points were then fit to an equation with the same form as eq 4, where here *c* is the EC_{50} for calcium-dependent protein binding and EC_{50} and N_h values were stored. This process was repeated 500 times for each protein state. The fits were then sorted by minimum sum of squared error (SSE), and the average and ±2 SD values were computed for the top 100 fits for each protein. Computed values were all near the values reported for the single best fit using the gathered data, which indicates the data values describe the system well and the fit values are robust. Clusters of all computed fit values are shown in **Figure S10** and clusters of the top 100 fits by SSE are shown in **Figure S11**.

Dissociation analysis We fit each protein variant's SPR dissociation traces to a single exponential of the form:

$$response(t) = a_x * e^{-k*t} + b_x \quad (5)$$

where *response(t)* is the response as a function of time, *t*, and *k* is the off rate. For each protein, *a* and *b* were allowed to vary per response, while all responses were simultaneously fit to a single shared off rate, *k*, that minimized the sum of squared errors (SSE) of the responses. Calcium concentrations less than 10 μM were removed from the fits, as their responses were not significantly above the noise threshold of the instrument.

For WT, the fit-determined off rate was $k_{wt} = 0.091$ sec^{-1}, for *trans* X-EC12, $k_{trans} = 0.075$ sec^{-1}, and for *cis* X-EC12, $k_{cis} = 0.072$ sec^{-1}. Because all traces for each protein could be fit to a single off rate using a single exponential fit, this indicates that we observed only one interacting species dissociating during the experiment. Dissociation traces, fits and example residuals are shown in **Figure S13.**

Size Exclusion Chromatography

We used size exclusion chromatography to show a decrease in X-EC12 homodimerization after illumination. Protein was diluted to a final concentration of 250 μM in TBS (25mM Tris pH 7.5, 150mM NaCl) at room temperature. For *trans* X-EC12, calcium was added to a final concentration of 2.5 mM and left to equilibrate for 5 minutes at room temperature, then 25 μL of protein was injected into a Superdex 75 PC 3.3/30 column (GE # 17-0771-01) equilibrated in TBS and attached to a 1200 Series HPLC (Agilent) at a flow rate of 100 μL/min. *Cis* X-EC12 was illuminated with a 1W UV LED (emission maximum 365 nm) for 6 minutes prior to the addition of calcium, after which it was treated the same as *trans*. Protein was detected by monitoring absorbance at 280 nm. We observed the expected decrease in the fraction of protein forming dimers after illumination, indicating that the *cis* X-EC12 homodimerization is weaker than that of *trans* X-EC12. Representative traces are shown in **Figure S12**.

References

(1) Rosetta- The premier software suite for macrommolecular modeling. http://www.rosettacommons.org (accessed May 16th 2013)
(2) Kortemme, T.; Baker, D. *Proc. Natl. Acad. Sci. USA* **2002**, *99*, 14116.
(3) Kortemme, T.; Kim, D.; Baker, D. *Sci. Signaling* **2004**, *2004*, pl2.

(4) Schrodinger, LLC 2013.
(5) Leckband, D.; Prakasam, A. *Annu Rev Biomed Eng* **2006**, *8*, 259.
(6) Harrison, O. J.; Bahna, F.; Katsamba, P. S.; Jin, X.; Brasch, J.; Vendome, J.; Ahlsen, G.; Carroll, K. J.; Price, S. R.; Honig, B.; Shapiro, L. *Nat. Struct. Mol. Biol.* **2010**.
(7) Harrison, O. J.; Corps, E. M.; Kilshaw, P. J. *J. Cell Sci.* **2005**, *118*, 4123.
(8) Koch, A.; Pokutta, S.; Lustig, A.; Engel, J. *Biochemistry* **1997**, *36*, 7697.
(9) Beckett, D.; Kovaleva, E.; Schatz, P. J. *Protein Sci.* **1999**, *8*, 921.
(10) Burns, D. C.; Zhang, F.; Woolley, G. A. *Nat. Protoc.* **2007**, *2*, 251.
(11) Gasteiger, E.; Gattiker, A.; Hoogland, C.; Ivanyi, I.; Appel, R. D.; Bairoch, A. *Nucleic Acids Res* **2003**, *31*, 3784.
(12) Zhang, Z.; Burns, D.; Kumita, J.; Smart, O.; Woolley, G. *Bioconj. Chem.* **2003**.
(13) Beharry, A. A.; Woolley, G. A. *Chem Soc Rev* **2011**, *40*, 4422.
(14) Woolley, G., University of Toronto, Toronto, ON Personal Communication, 2012.
(15) Courjean, O.; Chevreux, G.; Perret, E.; Morel, A.; Sanglier, S.; Potier, N.; Engel, J.; van Dorsselaer, A.; Feracci, H. *Biochemistry* **2008**, *47*, 2339.
(16) Peschke, M.; Verkerk, U. H.; Kebarle, P. *J Am Soc Mass Spectrom* **2004**, *15*, 1424.
(17) Weiss, J. N. *FASEB J.* **1997**, *11*, 835.